Supporting Information

A tri-(Ru^{II}-Gd_2^{III}) and tetranuclear (Ru^{II}-Gd_3^{III}) *d-f* Heterometallic Complexes as Potential Bimodal Imaging Probes for MRI and Optical Imaging

A. Nithyakumar and V. Alexander*

Department of Chemistry, Loyola College, Chennai-600034, India.

Table of Contents

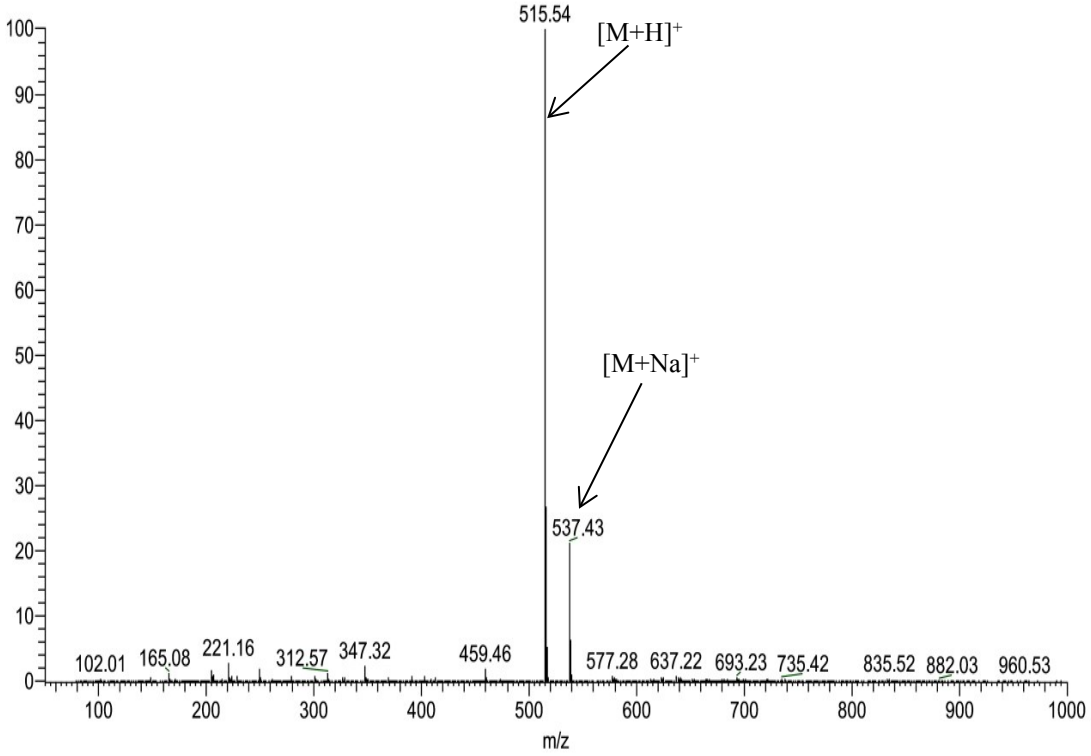

Figure S1. ESI mass spectrum of t-Bu-DO3A (**1**).

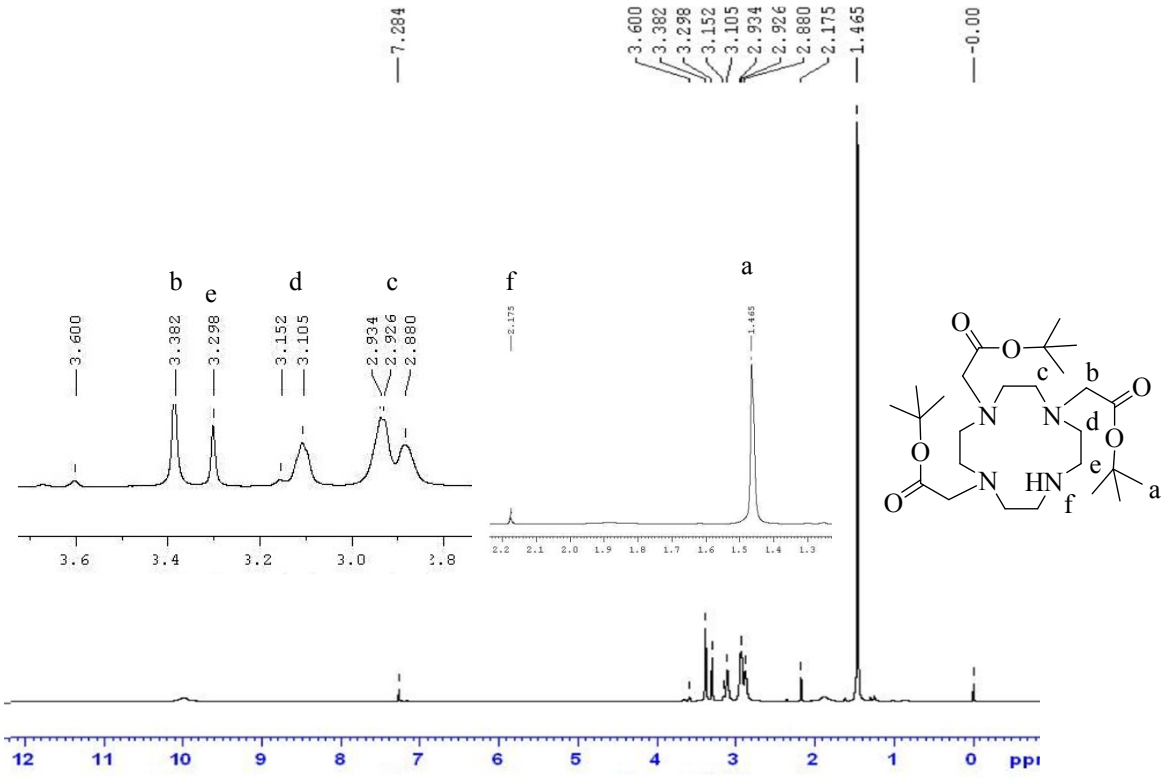

Figure S2. 400 MHz ^{1}H NMR spectrum of t-Bu-DO3A (**1**) in $CDCl_3$ at 25 ºC.

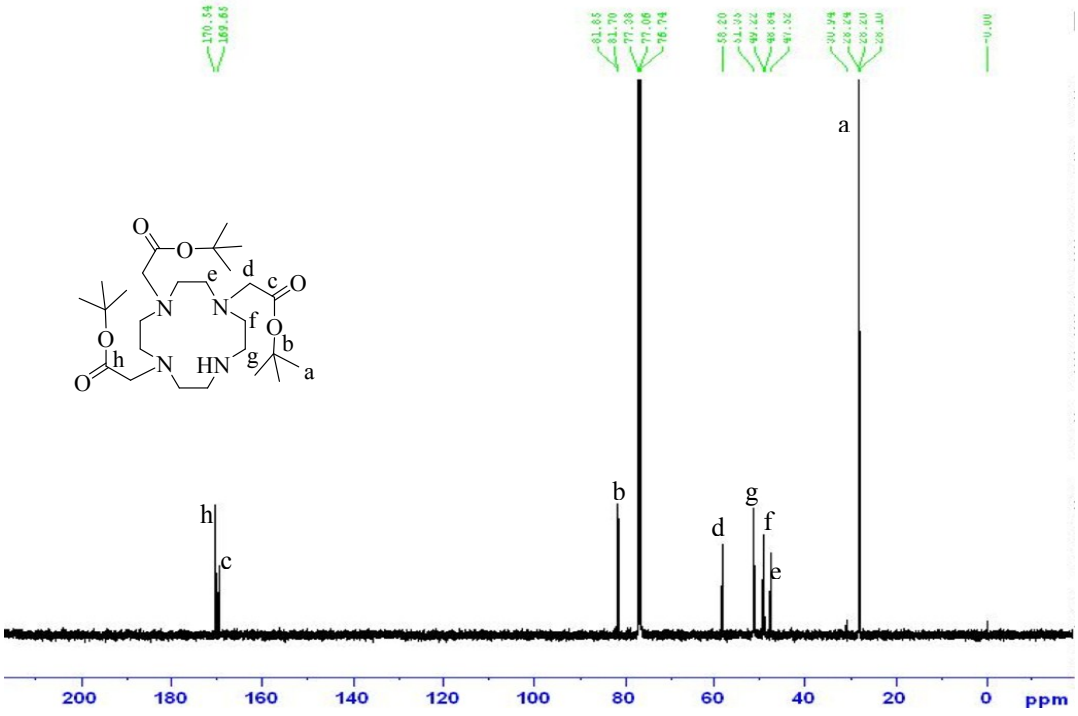
170.54
169.65
81.85
81.70
77.38
77.06
76.74
58.20
51.93
49.22
48.69
47.32
30.94
28.24
28.20
28.10
0.00
a
b
d
g
f
e
h
c
200
180
160
140
120
100
80
60
40
20
0
ppm

Figure S3. 100 MHz ^{13}C NMR spectrum of t-Bu-DO3A (**1**) in $CDCl_3$ at 25 ºC.

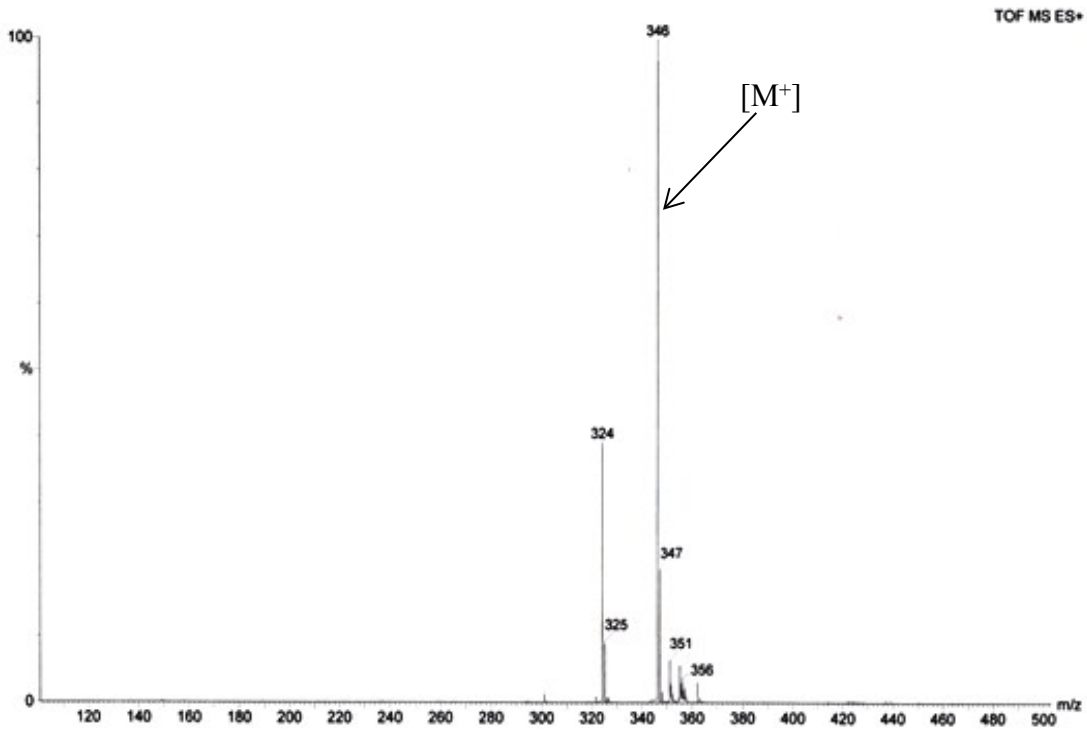

Figure S4. ESI mass spectrum of DO3A (**2**).

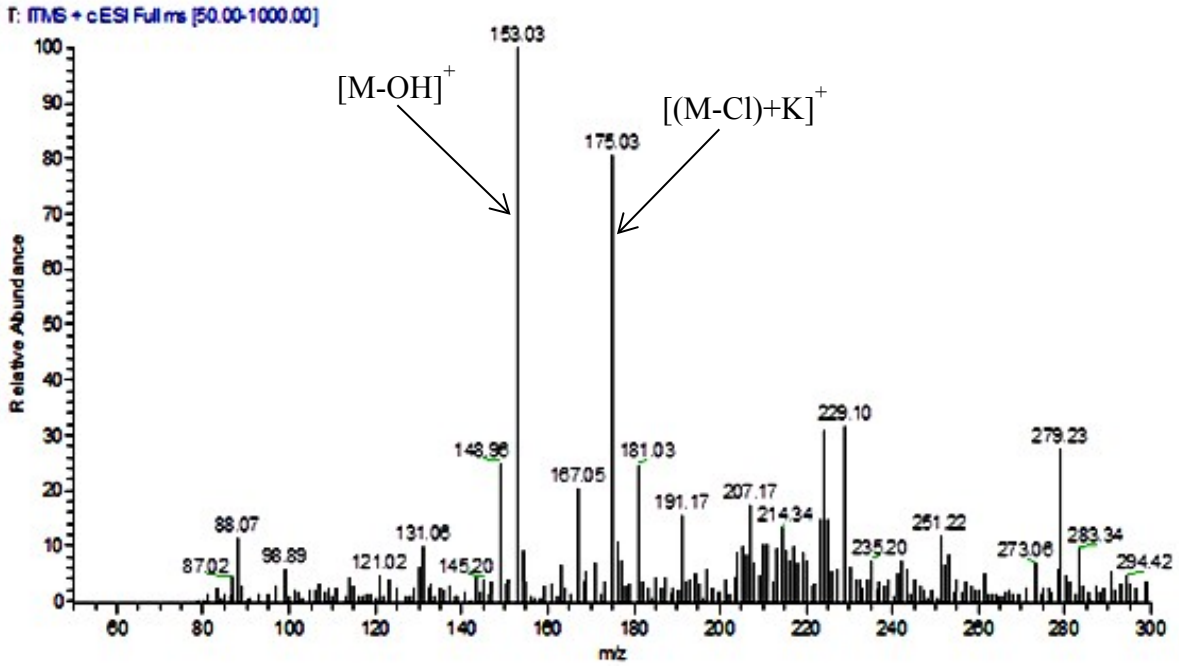

Figure S5. ESI mass spectrum of 2-chloro-*N*-(pyridine-4-yl)acetamide (**3**).

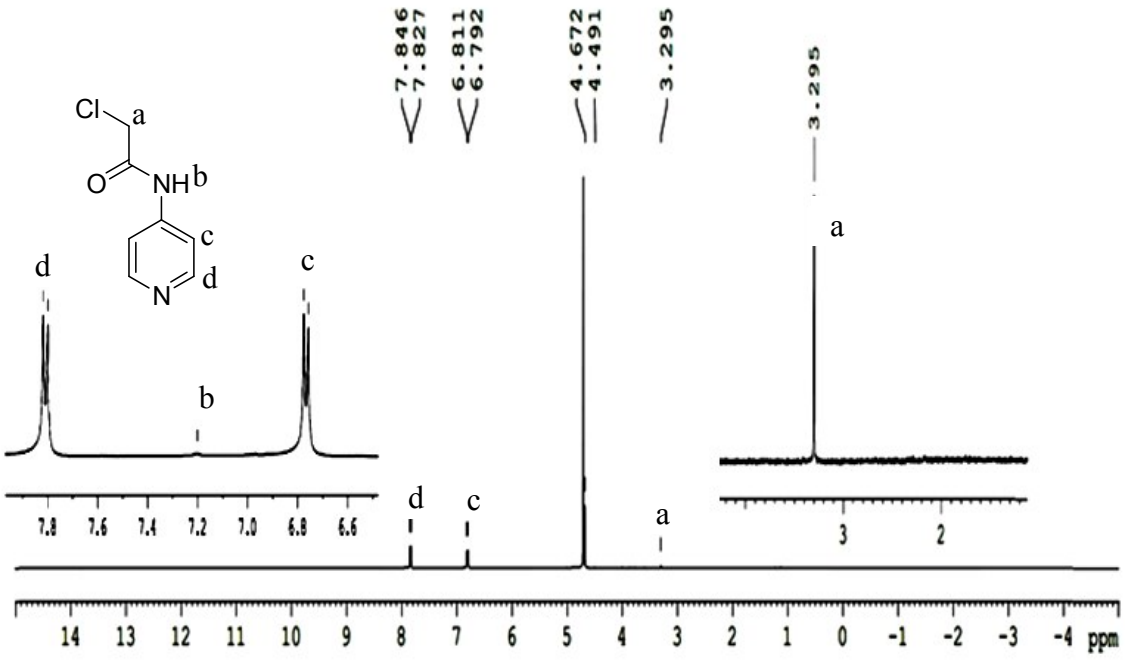

Figure S6. 400 MHz ^{1}H NMR spectrum of 2-chloro-*N*-(pyridine-4-yl)acetamide (**3**) in D_2O at 25 °C.

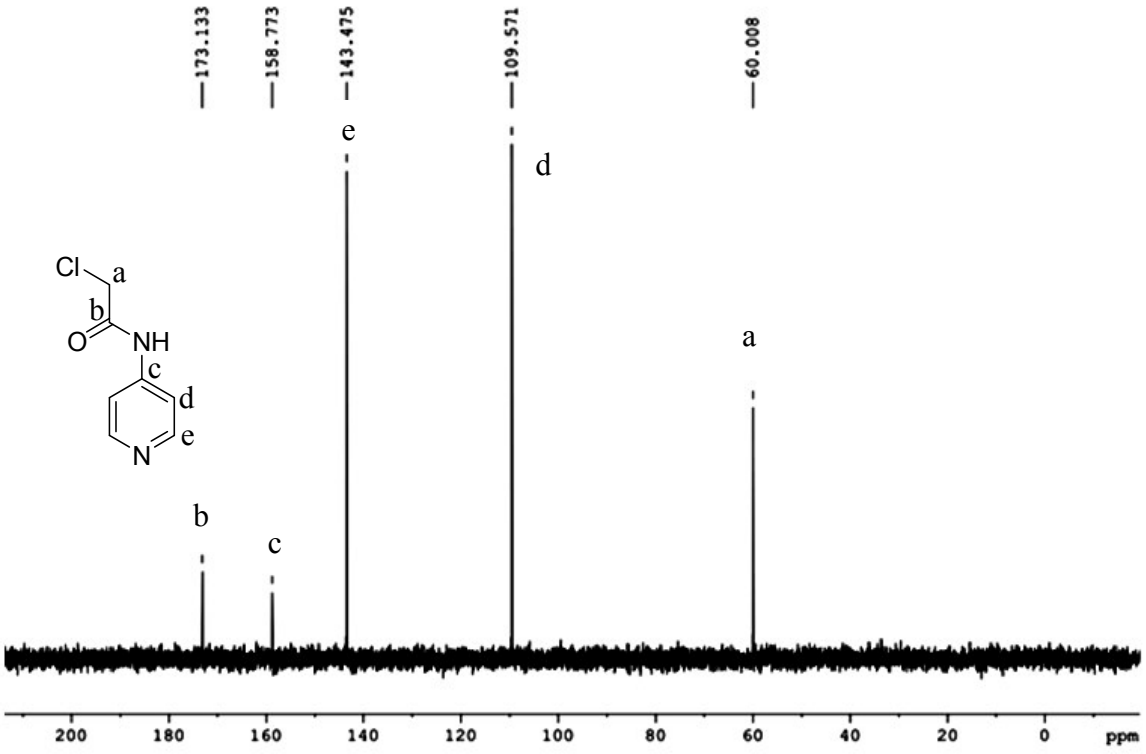

Figure S7. 100 MHz ^{13}C NMR spectrum of 2-chloro-*N*-(pyridine-4-yl)acetamide (**3**) in D_2O at 25 °C.

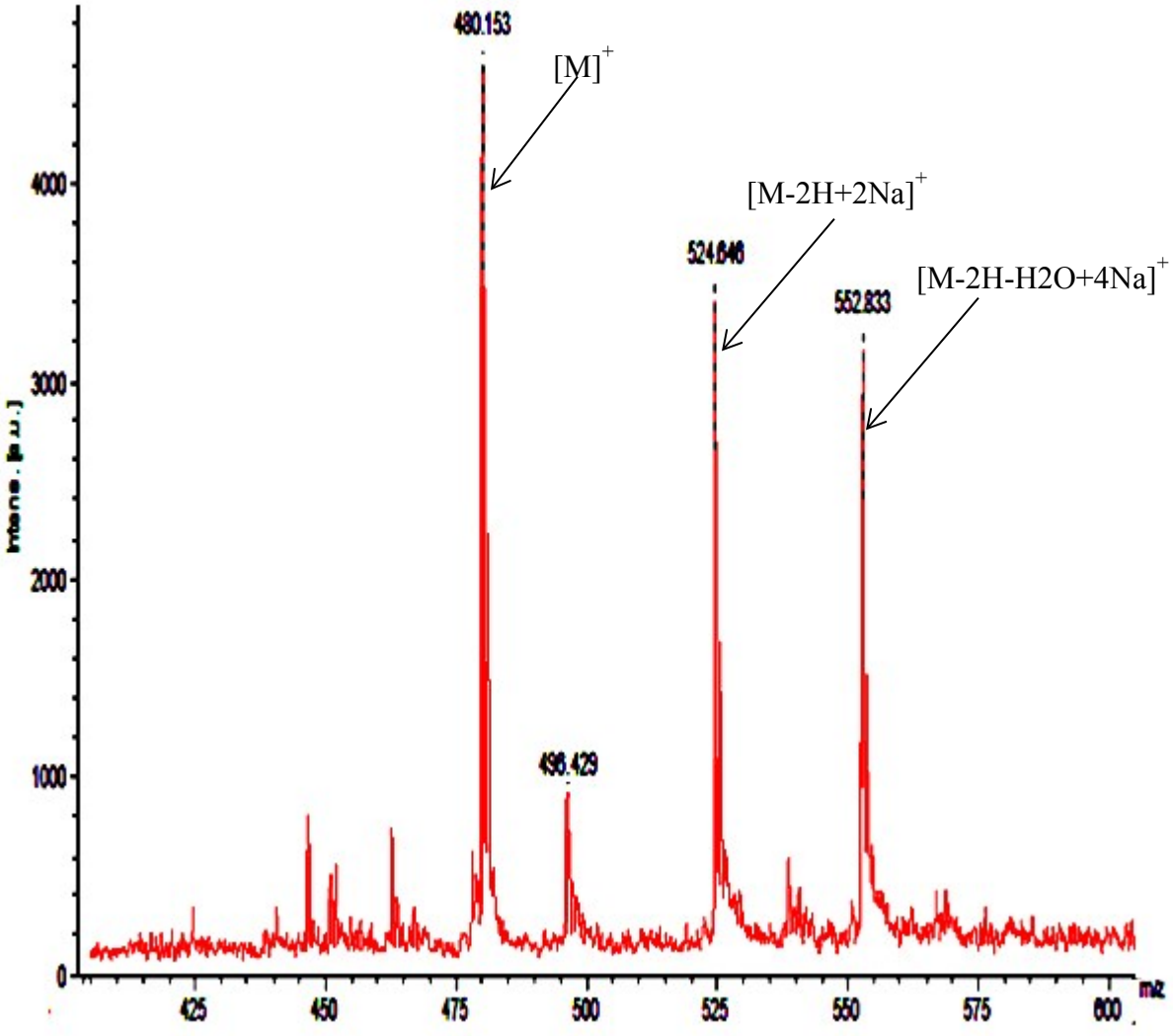

Figure S8. MALDI-TOF mass spectrum of DOTA-AMpy (**4**).

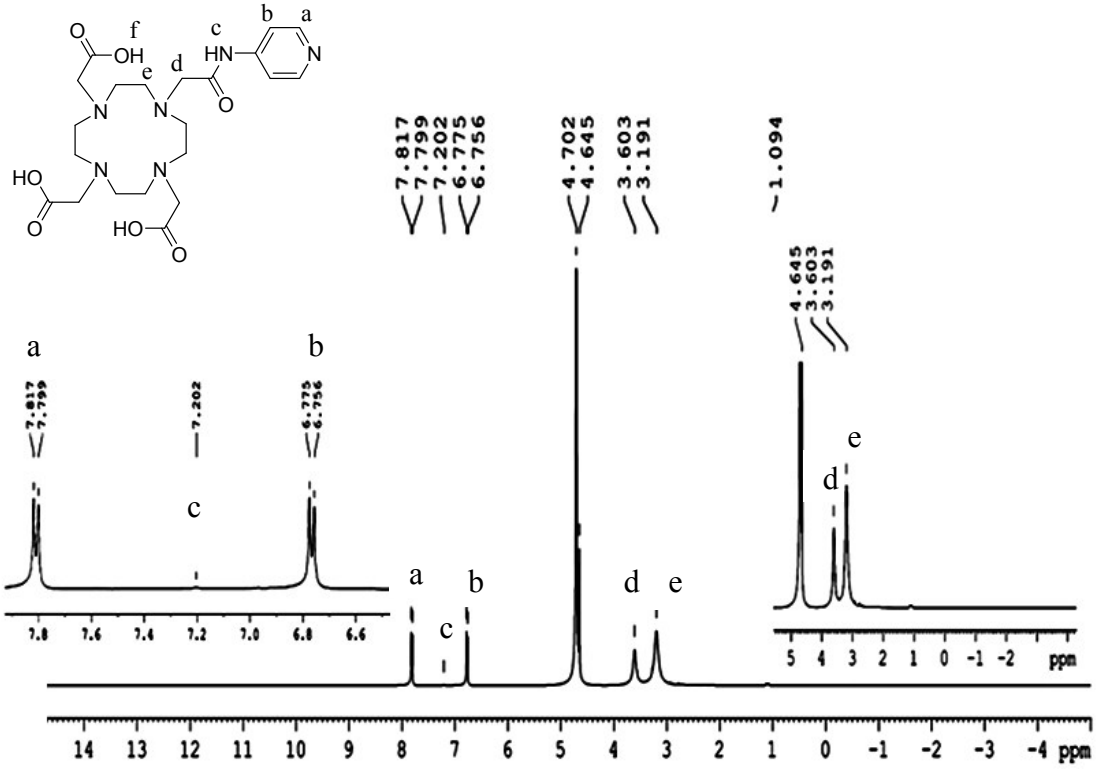

Figure S9. 400 MHz ^{1}H NMR spectrum of DOTA-AMpy (**4**) in D_2O at 25 °C.

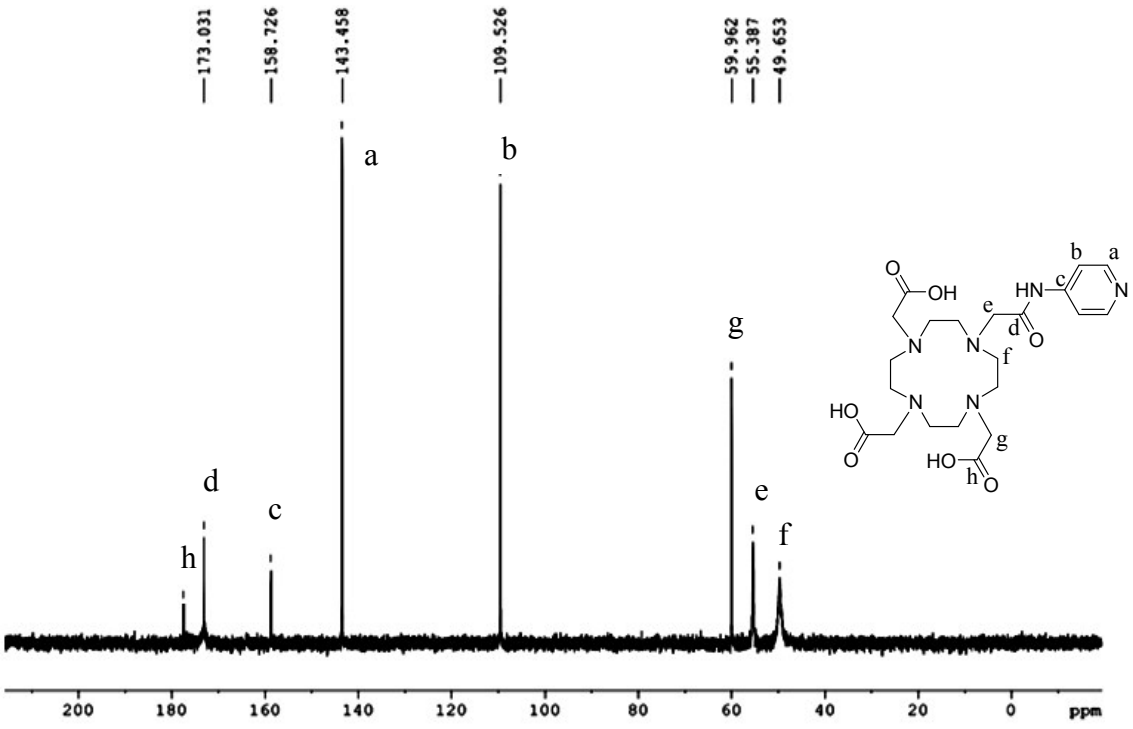

Figure S10. 100 MHz ^{13}C NMR spectrum of DOTA-AMpy (**4**) in D_2O at 25 °C.

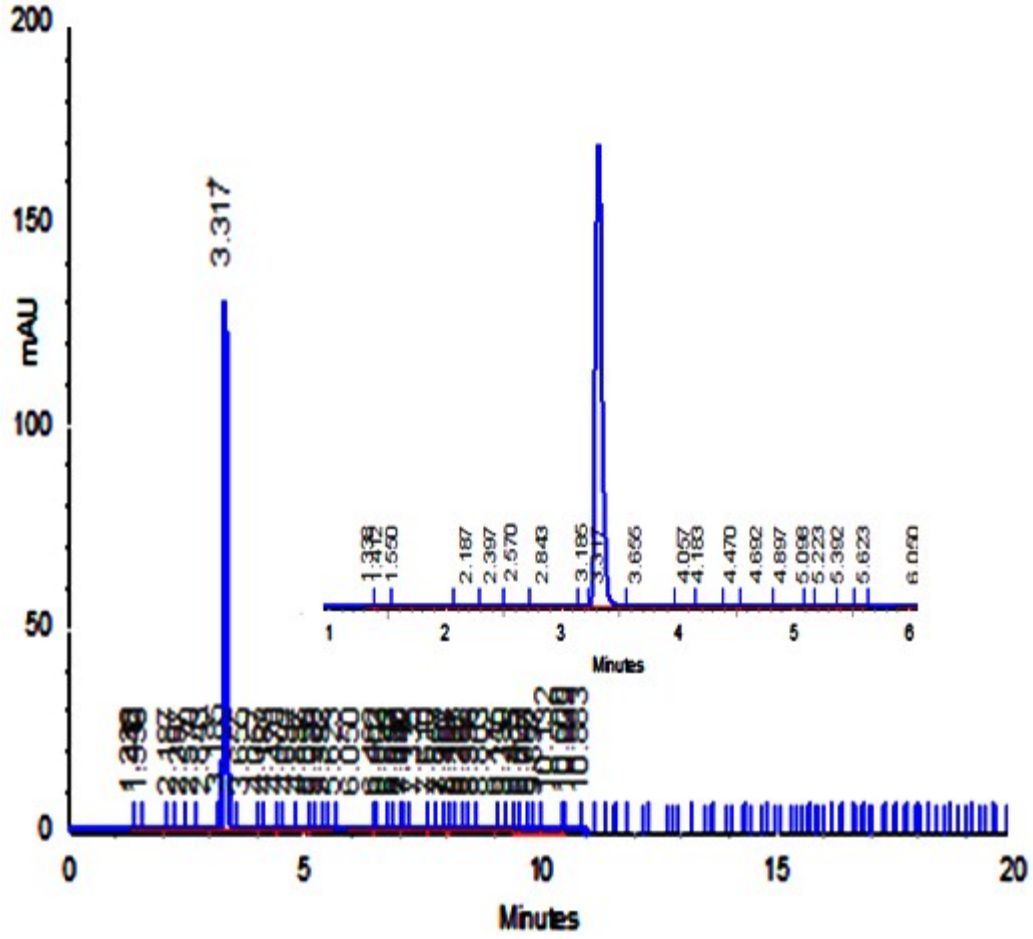

Figure S11. High performance liquid chromatogram of DOTA-AMpy (**4**) (t_R = 3.31 min). Inset: expansion of chromatogram of **4**.

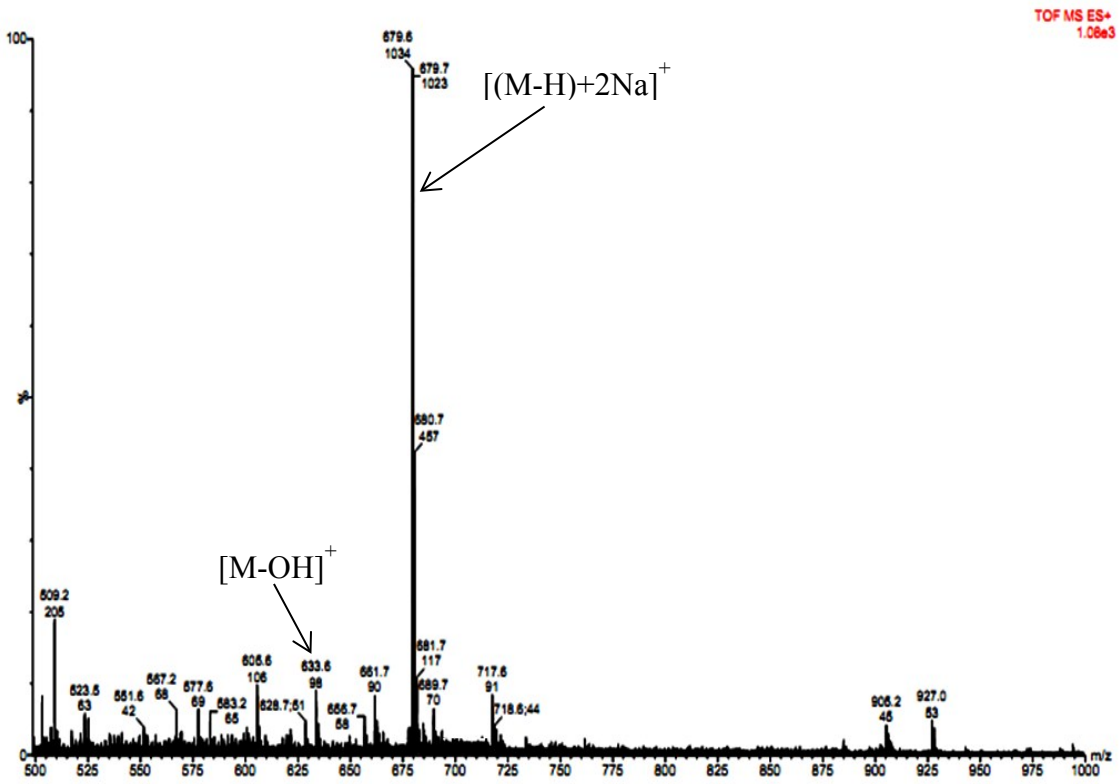
TOF MS ES+
1.06e3
100
%
0
679.6
1034
679.7
1023
[(M-H)+2Na]+
680.7
457
[M-OH]+
509.2
205
623.5
63
551.6
42
557.2
68
577.6
69
583.2
65
605.6
106
628.7;51
633.6
99
656.7
56
661.7
90
681.7
117
689.7
70
717.6
91
718.6;44
906.2
45
927.0
53
500
525
550
575
600
625
650
675
700
725
750
775
800
825
850
875
900
925
950
975
1000
m/z

Figure S12. ESI mass spectrum of [Gd(DOTA-AMpy)(H_2O)] (**5**).

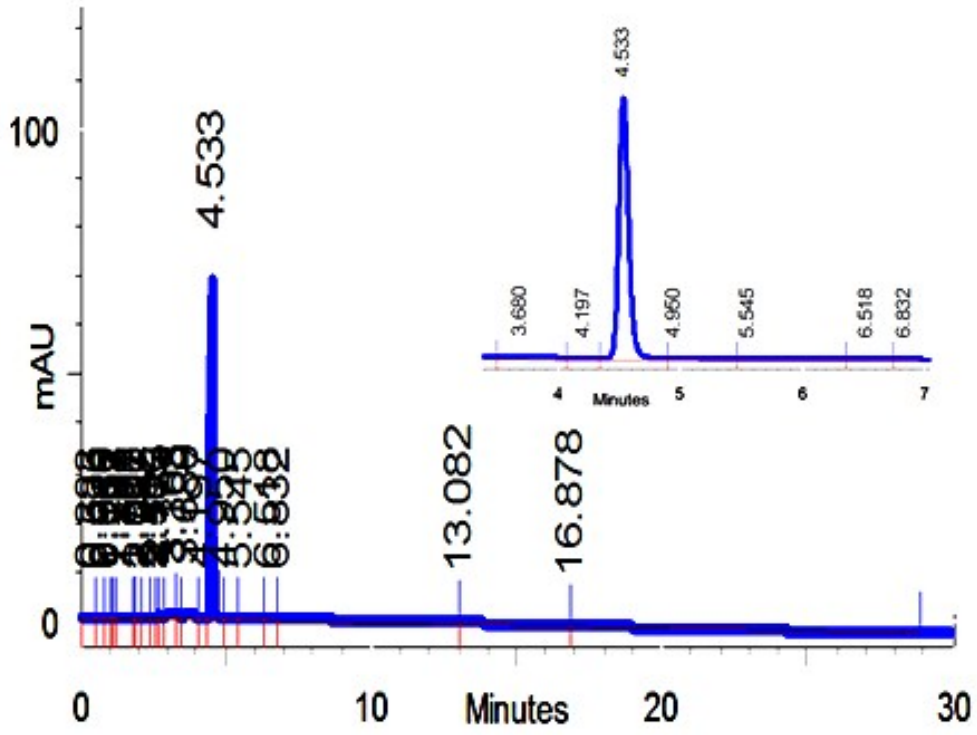

Figure S13. High performance liquid chromatogram of [{Ru(phen)$_2${Gd(DOTA-AMpy)(H_2O)}$_2$]Cl_2 (**7**) (t_R = 4.53 min); inset: expansion of the chromatogram.

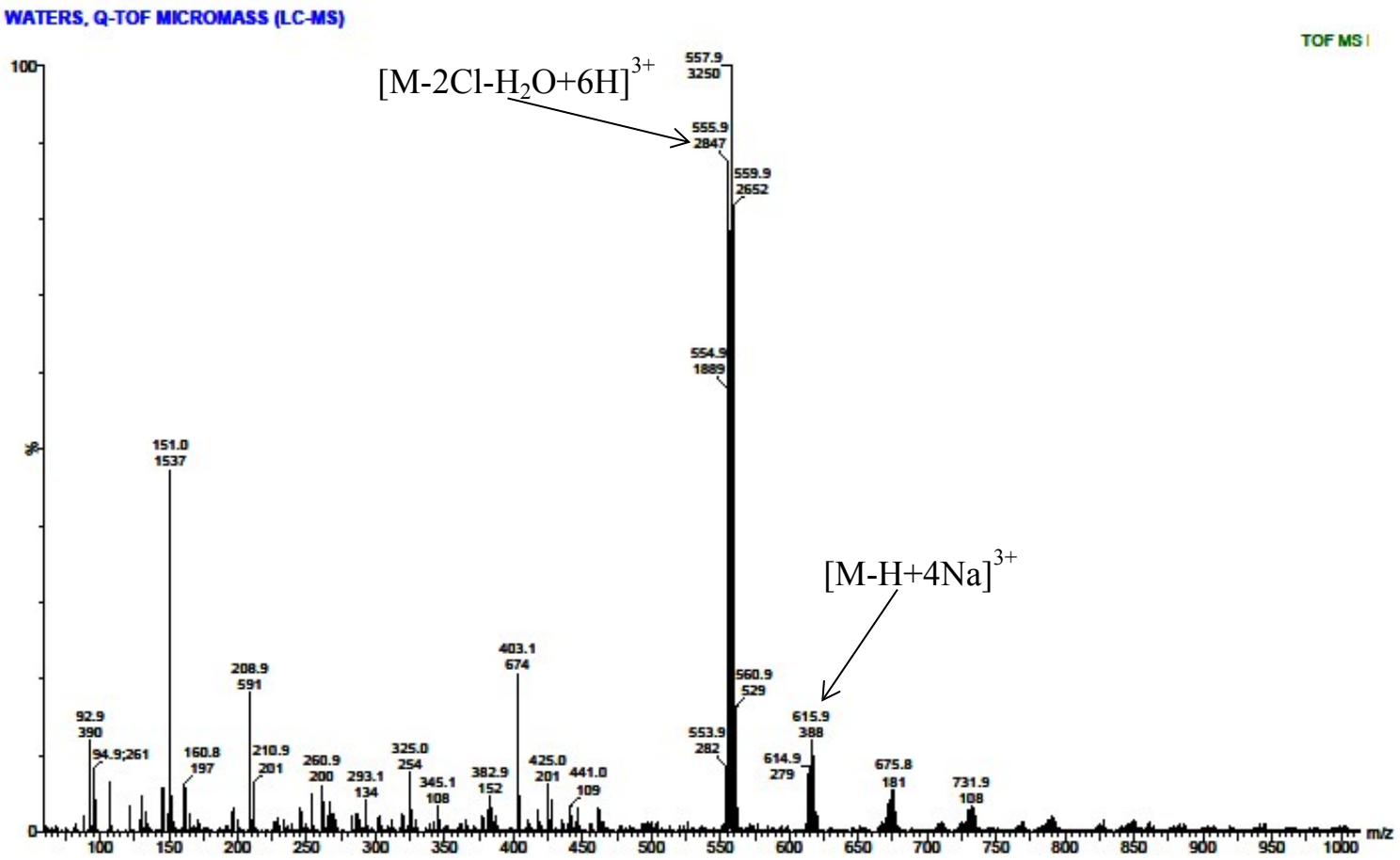

Figure S14. ESI-TOF mass spectrum of [{Ru(phen)$_2$}{Gd(DOTA-AMpy)(H$_2$O)}$_2$]Cl$_2$ (**7**).

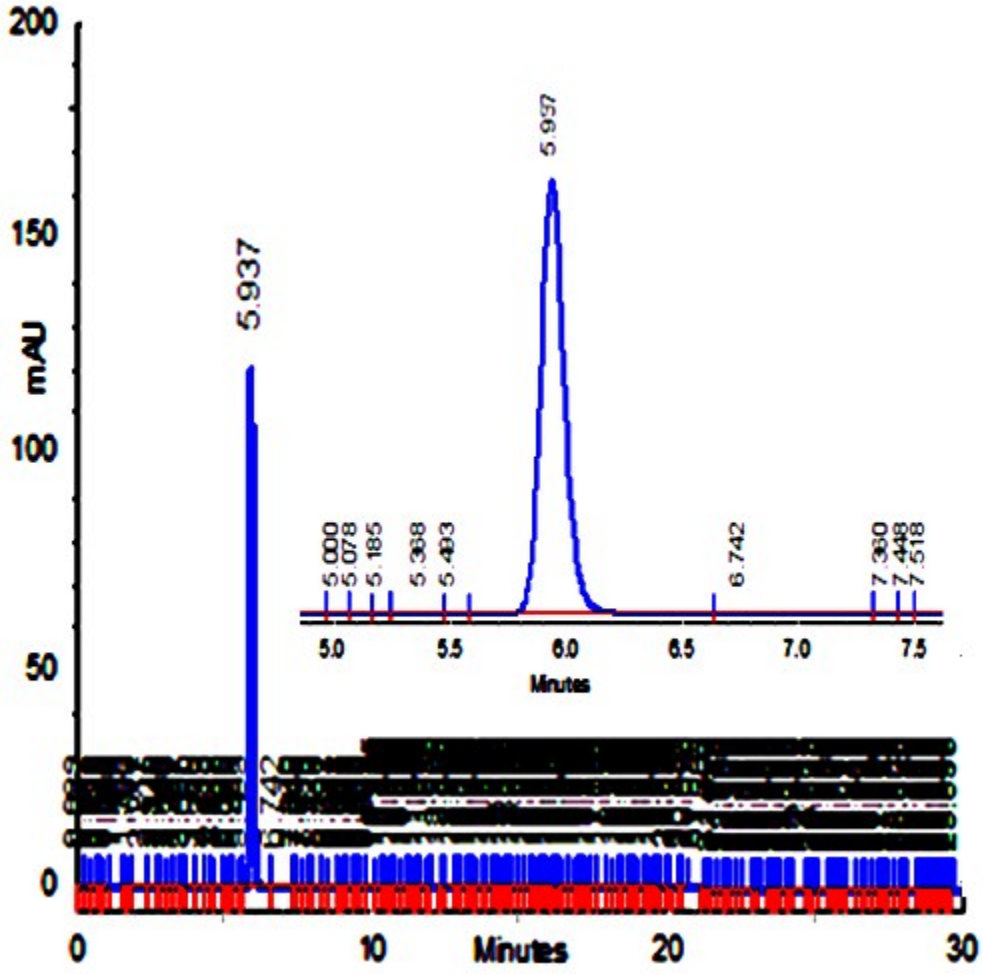

Figure S15. High performance liquid chromatogram of [Ru(ttpy){Gd(DOTA-AMpy)(H_2O)}$_3$]Cl_2 (**9**) (t_R = 5.93 min); inset: expansion of the chromatogram.

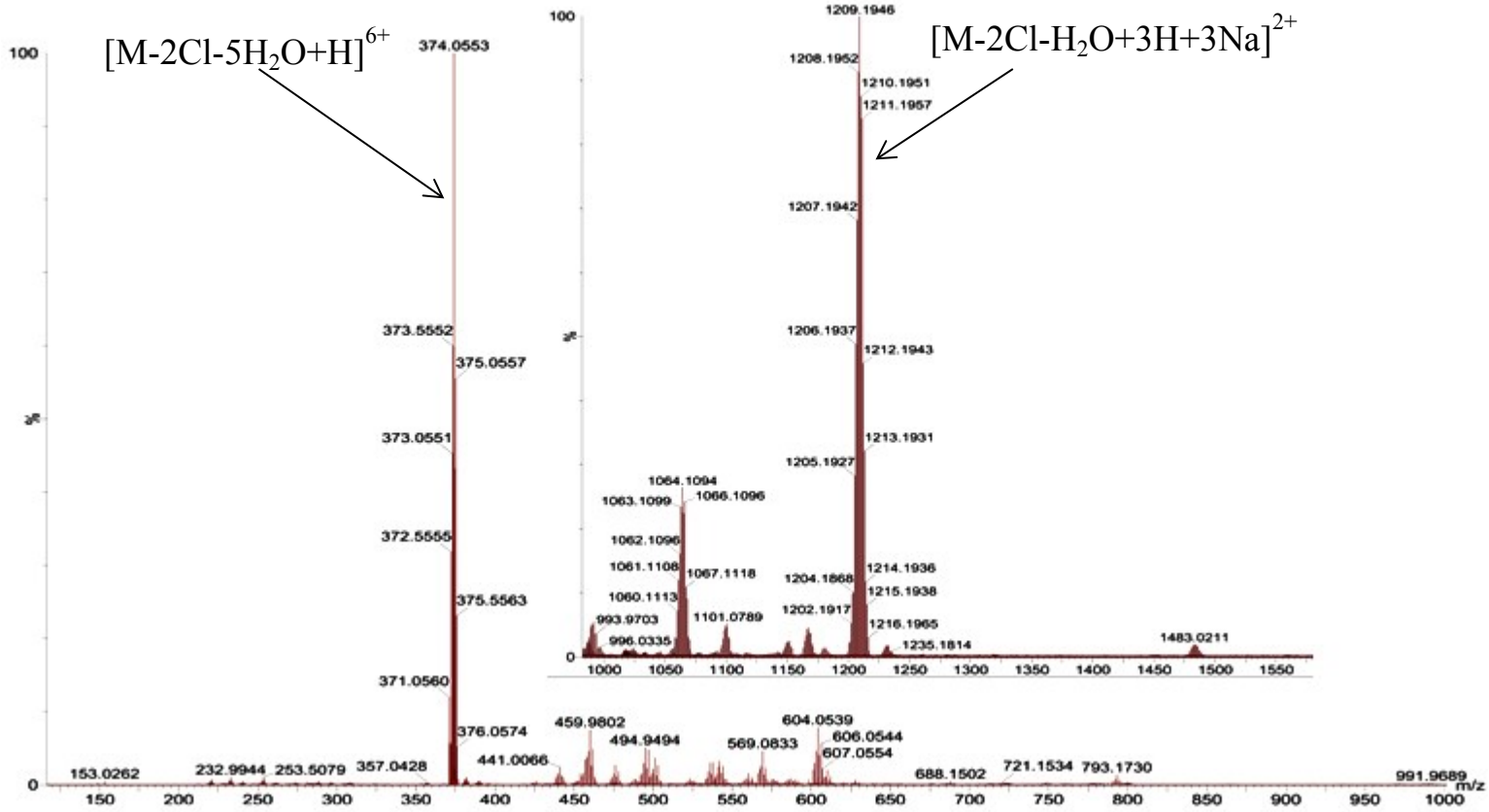

Figure S16. ESI-TOF mass spectrum of [Ru(ttpy){Gd(DOTA-AMpy)(H_2O)}$_3$]Cl_2 (**9**).

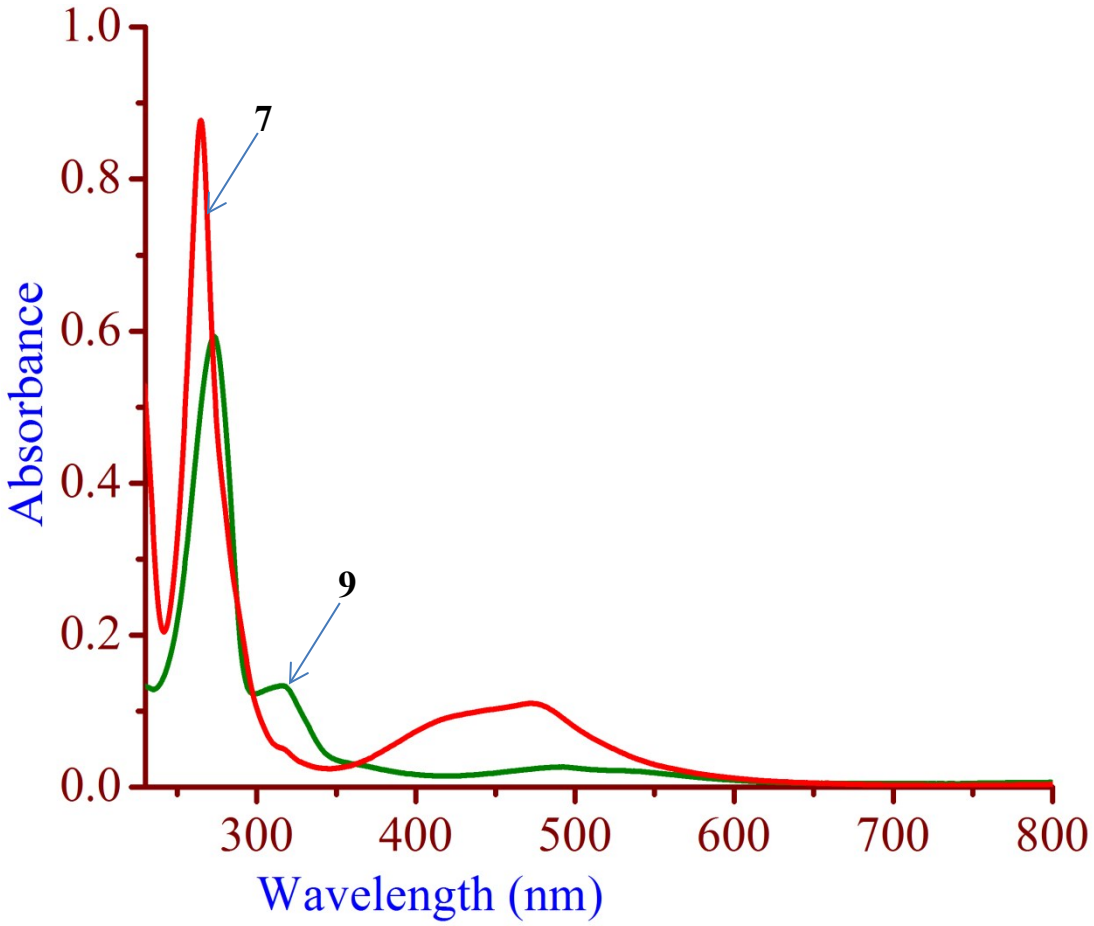

Figure S17. Electronic absorption spectra of [{Ru(phen)$_2${Gd(DOTA-AMpy)(H$_2$O)}$_2$]Cl$_2$ (**7**) and [Ru(ttpy){Gd(DOTA-AMpy)(H$_2$O)}$_3$]Cl$_2$ (**9**) in 0.1 M Tris-HCl buffer, pH = 7.4 at 25 °C.

complex	1 μM	10 μM	25 μM	50 μM
[{Ru(phen)$_2${Gd(DOTA-AMpy)(H$_2$O)}$_2$]Cl$_2$ **7**)	93.2	77.3	49.2	19.5
[Ru(ttpy){Gd(DOTA-AMpy)(H$_2$O)}$_3$]Cl$_2$ (**9**)	88.5	68.3	38.6	16.5

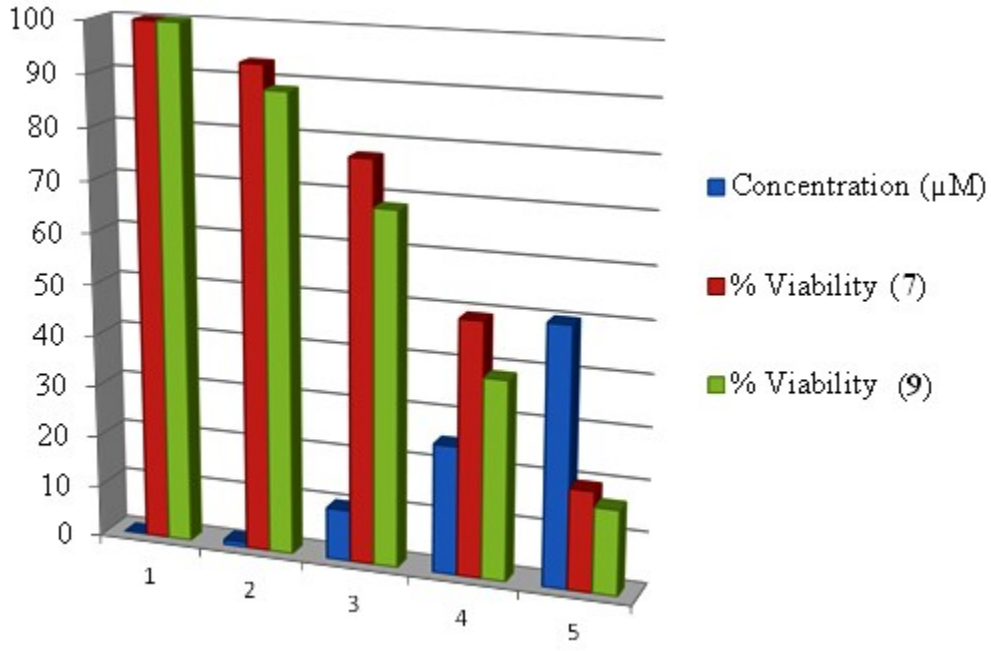

Figure S18. Concentration versus viability plot of incubated HeLa cell lines with varying concentration of [{Ru(phen)$_2${Gd(DOTA-AMpy)(H$_2$O)}$_2$]Cl$_2$ (**7**) and [Ru(ttpy){Gd(DOTA-AMpy)(H$_2$O)}$_3$]Cl$_2$ (**9**) for 24 h at 37 ºC: (1) control, (2) 1 μM, (3) 5 μM, (4) 25 μM and (5) 50 μM.

Table S1. Electronic Absorption Spectral Data of $[Ru(phen)_2\{Gd(DOTA\text{-}AMpy)(H_2O)\}_2]Cl_2$ (7) and $[Ru(ttpy)\{Gd(DOTA\text{-}AMpy)(H_2O)\}_3]Cl_2$ (9) in 0.1 M Tris-HCl Buffer, pH = 7.4 at 25 °C (6×10^{-6} M)

complex	λ_{max} (nm)	ε ($dm^3\ mol^{-1}\ cm^{-1}$)	assignment
$[Ru(phen)_2\{Gd(DOTA\text{-}AMpy)(H_2O)\}_2]Cl_2$ (**7**)[a]	265	146,166	LC ($\pi \rightarrow \pi^*$)
	473	18,333	^{1}MLCT ($d \rightarrow \pi^*$)
$[Ru(ttpy)\{Gd(DOTA\text{-}AMpy)(H_2O)\}_3]Cl_2$ (**9**)[b]	272, 317	98,333, 22,166	LC ($\pi \rightarrow \pi^*$)
	493	4333	^{1}MLCT ($d \rightarrow \pi^*$)

[a] *Inorg. Chem*. 2011, **50**, 10005-10014.
[b] *Inorg. Chem*. 1984, **23**, 2236-2242.

Table S2. Intercalation data of $[Ru(phen)_2\{Gd(DOTA\text{-}AMpy)(H_2O)\}_2]Cl_2$ (7) and $[Ru(ttpy)\{Gd(DOTA\text{-}AMpy)(H_2O)\}_3]Cl_2$ (9) with DNA (PDB ID: 1BNA; Q-Site Finder) and Preferential Binding Site from the Docked Structure

complex	DNA (PDB ID: 1BNA) sequence A	position	binding site	distance (Å)	type of bonding	complementary score
$[Ru(phen)_2\{Gd(DOTA\text{-}AMpy)(H_2O)\}_2]Cl_2$ (**7**)	CGCGAATTCGCG	G4′	O	1.84	hydrogen	4870
	CGCGAATTCGCG	C3′	O	2.05	hydrogen	
$[Ru(ttpy)\{Gd(DOTA\text{-}AMpy)(H_2O)\}_3]Cl_2$ (**9**)	CGCGAATTCGCG	C7′	H	-	-	6250
	CGCGAATTCGCG	C6′	C	-	-	

Table S3. Molecular Docking Data of the Binding of $[Ru(phen)_2\{Gd(DOTA\text{-}AMpy)(H_2O)\}_2]Cl_2$ (7) and $[Ru(ttpy)\{Gd(DOTA\text{-}Ampy)(H_2O)\}_3]Cl_2$ (9) with HSA (PDB ID: 1h9z; Q-Site Finder)

complex	Human Serum Albumin (PDB ID: 1h9z) *residue*	*position*	binding site	distance (Å)	Type of bonding	docking energy (kcal/mol)
$[Ru(phen)_2\{Gd(DOTA\text{-}AMpy)(H_2O)\}_2]Cl_2$ (**7**)	THR 161	OH	N	3.12	Hydrogen	-466.84
	PHE 134	O	O	3.47	Hydrogen	
	SER 517	OG	C	3.45	Hydrogen	
$[Ru(ttpy)\{Gd(DOTA\text{-}AMpy)(H_2O)\}_3]Cl_2$ (**9**)	ARG 186	O	H	2.96	Hydrogen	-476.85
	HIS 146	NE2	N	3.51	Hydrogen	